# A Combined First Principles and Kinetic Monte Carlo study of Polyoxometalate based Molecular Memory Devices

P. Lapham, O. Badami, C. Medina-Bailon, F. Adamu-Lema, T. Dutta, D. Nagy, V. Georgiev and A. Asenov
Device Modelling Group
James Watt School of Engineering
University of Glasgow, Glasgow G12 8QQ, United Kingdom
E-mail: vihar.georgiev@glasgow.ac.uk

***Abstract*--In this paper, we combine Density Functional Theory with Kinetic Monte Carlo methodology to study the fundamental transport properties of a type of polyoxometalate (POM) and its behaviour in a potential flash memory device. DFT simulations on POM molecular junctions helps us demonstrate the link between underlying electronic structure of the molecule and its transport properties. Furthermore, we show how various electrode-molecule contact configurations determine the electron transport through the POM. Also, our work reveals that the orientation of the molecule to the electrodes plays a key role in the transport properties of the junction. With Kinetic Monte Carlo we extend this investigation by simulating the retention time of a POM-based flash memory device. Our results show that a POM based flash memory could potentially show multi-bit storage and retain charge for up to 10 years.**

## INTRODUCTION

Molecular electronics is an exciting interdisciplinary field that is attempting to overcome the inherent limit of miniaturization of conventional CMOS electronic devices [1]. One of the main challenges in fabricating commercial molecular electronic devices is a lack of fundamental understanding of quantum transport at the molecular level [2]. Using first principle methods and higher-level device simulation techniques the transport properties of molecules and realistic molecular devices can be understood further [3]. One such potential molecular device is based on Wells-Dawson Polyoxometalates (POMs). Due to their extremely small size and the fact they are highly redox active, POMs are being explored for potential use as the charge storage component in flash memory [4]. In addition to their size and redox properties, the fact that they are oxygen rich suggest they will have good compatibility with the CMOS fabrication process [5]. They are also thermally stable allowing for the device fabrication and operation [6].

Much of the previous work has focused on high level device simulation of POM based devices. The aim of this work is to fundamentally understand the transport properties of a POM molecule and link its underlying electronic structure to the current flow (electron transport). The most extensively studied single molecule device, both theoretically and experimentally, is the molecular junction where a single molecule is placed between two metal contacts. For that reason, gold-POM-gold (Au-POM-Au) devices were studied using Density Functional Theory (DFT).

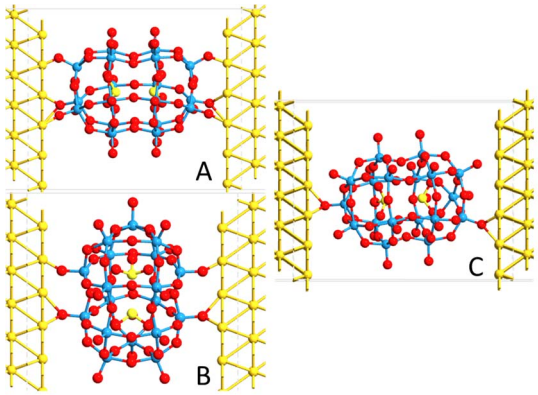


Figure 1. Au-POM-Au molecular junctions with different orientations (A&C vs B) and different number of contacts. The POM molecule is [W18O54(SO3)2]-4 where S=Yellow, W=Blue and O=Red.

in combination with non-equilibrium Green's function (NEGF) to explore the electron transport properties of a specific POM molecule, $[W_{18}O_{54}(SO_3)_2]^{-4}$.

Finally, to assess the use of POM molecules as the charge storage component in a flash cell, the retention time of a realistic POM-based flash cell is investigated using Kinetic Monte Carlo (KMC) approach. Some important input parameters (such as energy positions of molecular levels) are taken from DFT, thus this work combines both simulation methodologies.

## SIMULATION METHODOLOGY

In this work the simulations on the POM molecular junctions are carried out using DFT in combination with NEGF approach as implemented by QuantumATK-2018.06 software [7]. To accurately describe the electronic properties of the molecule, SGGA.BP86 functional was employed as it has been shown to successfully describe POMs in previous publications [8]. The SG15 pseudopotential and a medium basis set - comparable to DZP (Double Zeta Polarised)- were also used and satisfactorily reproduced the geometry and electronic properties of $[W_{18}O_{54}(SO_3)_2]^{-4}$ [4],[7],[9]. Due to computational cost, SZP (Single Zeta Polarised) basis-set was used to adequately describe the gold electrodes.

The geometry of the molecule was optimized in vacuum and the energy levels calculated using DFT. The devices were then built by placing the geometrically optimized POM cluster between two Au electrodes which are used as source and drain contact. In this way we were able to calculate the current flow in the POM molecule using NEGF computational method. Finally, a drain bias was applied incrementally between -1.5V

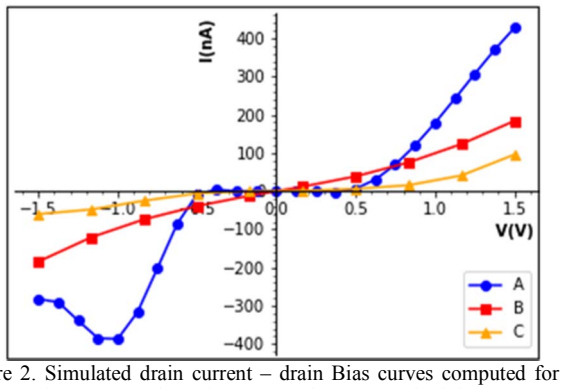


Figure 2. Simulated drain current – drain Bias curves computed for all configurations: A,B and C using DFT and NEGF methodology.

to +1.5V for all devices and the transmission spectra and current at each bias point were calculated.

The retention time was studied using Kinetic Monte Carlo (KMC) module of the in-house simulator – NESS[10],[11]. The molecule's energy levels and geometry obtained from the DFT calculations were used as input parameters for NESS. The KMC module calculates the changes in threshold voltage ($V_T$) due to the emission of electrons as a function of time. The KMC simulations were repeated 75 times to capture the statistical variability of the device.

## RESULTS AND DISCUSSION

One of the biggest challenges in the field of molecular electronics is the lack of detail at the atomic level. The current approach for theoretically studying molecular junctions is to simulate several reasonable junction geometries to gain an average picture of a realistic device where there are intrinsic geometric changes in the environment [12]. The geometry and bonding of the molecule to the electrode/surface largely dictates the transport properties of molecular devices [13].

Fig. 1 shows three different of many possible configurations for the molecular junctions aimed at probing the effect of molecule orientation and contact with the gold electrodes. The working models show the bulk electrodes act as a "reservoir of electrons" whilst the transport properties are dominated by the molecule and its connection to the electrodes.

The drain current - drain voltage ($I_D$-$V_D$) characteristics of all configurations have been calculated between the bias of -1.5V and +1.5V and are illustrated in Fig. 2. Using the Landauer-Buttiker formalism combined with NEGF and DFT approaches, the theoretical transmission spectra for the three different configurations presented in Fig.1 can be calculated. These are shown in Fig.3 at zero drain bias.

The transmission spectrum highlights energies at which electrons can pass through the system via scattering and describes the probability of this transmission T(E). The computed spectra are also linked with the underlying symmetry of the molecular orbitals of the POM cluster. The position of each transmission peak corresponds to the conduction channel and hence molecular orbital. For instance, the first peak above the Fermi level ($E_f$=0.0 eV) is directly linked to the Lowest

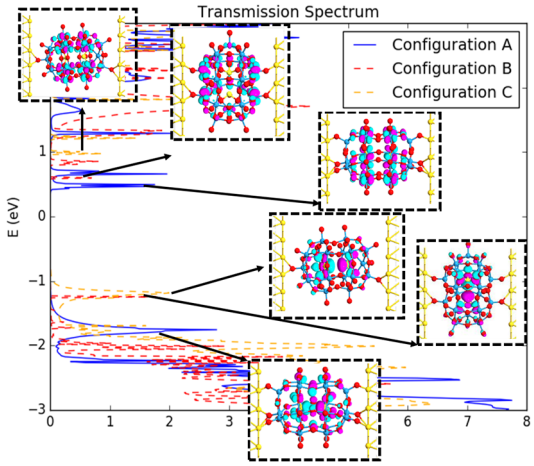


Figure 3. Transmission spectra for the three molecular junction configurations computed using the combination of DFT and NEGF

Unoccupied Molecular Orbital (LUMO). The peak below the $E_f$ is due to the Highest Occupied Molecular Orbital (HOMO).

The coupling of the molecule to the electrodes in the molecular junction results in a shift in the position of the energy levels compared to the isolated molecule. Depending on the strength of the coupling, the discrete energy levels are broadened into band-like states. This broadening affects the transmission coefficient which correspond to a discrete energy level(or levels) of the molecule [14].

Fig. 3 shows how the intensity of the peaks at similar energies are significantly different for each configuration. This highlights the impact that contact geometry and the strength/number of contacts between the molecule and electrodes has on the transport. The bonding between the molecule and the electrode determines how the molecular energies are distorted and hence influences the transmission coefficients of the POM junctions.

Another important feature is the lack of peaks between -1eV and 1eV which corresponds to the HOMO-LUMO gap of the molecule. This gap influences the electron transport properties of the device with larger gaps resulting in insulator-like properties. In addition, the symmetry of the HOMO-LUMO levels-in the device- have a very similar profile as those of the isolated molecule in vacuum [4].

The $I_D$-$V_D$ curves presented in Fig. 2 are consistent with the computed transmission spectra shown in Fig.3. Clearly, configuration A has higher drain current as compared to B and C. This is because, in configuration A, the POM cluster has six oxygen atoms in direct contact to the gold electrodes, whereas configurations B and C have four and two, respectively (please see Fig. 1). Larger contact area between the molecule and the electrodes leads to more conduction channels and hence higher probability for charge transport between the source and the drain.

The contact geometry of A seems to favorably align the HOMO and LUMO peaks within the bias window resulting in considerably higher current than configurations B & C. In addition, the "horizontal" geometry of A & C suggests better

alignment of the transmission peaks as their intensity (T(E)) are higher than that of B. This is visualized in the electron density difference calculations in Fig. 4. The electron density difference was calculated and visualized for the three configurations by subtracting the values of the electron density at drain bias 1.5V and at 0.0V. The differences are visualized with the same isovalues.

It is evident from Fig.4 the following assertions. Firstly, the difference in electron density is the most pronounced at the drain side (right hand side is the drain electrode) hence where there is the maximum change of the charge. This can be directly linked to the most probable conduction pathways. Secondly, structure A shows the biggest clouds of the electron density difference hence the movement of electrons from source to drain is bigger than that for B and C which is consistent with the $I_D$-$V_D$ curves in Fig.2.

Thirdly, Fig.4b highlights the link between the molecule's discrete energy levels and the transport. The blue surface represents where the density has moved from and is centered around the $SO_3^{2-}$ moieties, which resembles the structure of the HOMO. This is a strong indication that the movement of electrons from the source to the drain is predominately dominated by the HOMO level which has the same symmetry and shape as in the isolated POM molecule.

When a bias is applied across a molecular junction, the transmission peaks are shifted to higher energy with increased drain bias. Fig. 5 gives insight to how the transmission spectra changes under drain bias for configuration A. The blue line represents the drain bias window. The spectrum with no blue line represents zero bias transmission. From top to bottom the drain bias goes from -2.0V, -1.5V, -1.0V -0.5V 0.0V, 0.5V, 1.0V, 1.5V, 2.0V. The figure demonstrates how the intensity of the transmission peaks decrease within the bias window. As a result, the change in the transmission spectra with increased applied bias explains why less current flows than expected from the zero-bias transmission spectra.

Fig. 5 also provides an insight to why the current decreases between the bias of -1V to -1.5V. The intensity of the peaks at a bias of -1V is higher than that of the peaks in -1.5V. The current has been calculated over a larger energy window and so the current goes down. This is consistent with the Landauer formalism for calculating current [15].

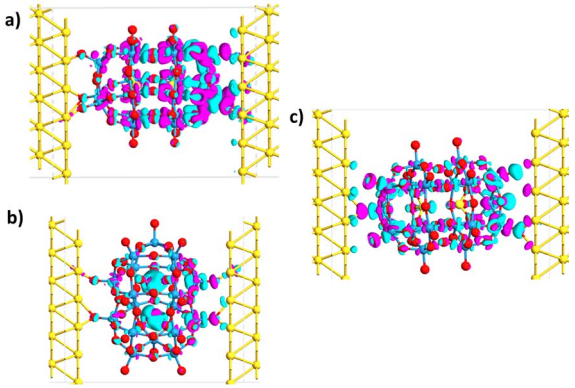


Figure 4. Electron density difference for the A, B and C configurations. Illustrating the change in electron density from 0.0V drain bias to 1.5V. (Isovalues= 0.0004 e/bohr$^3$)

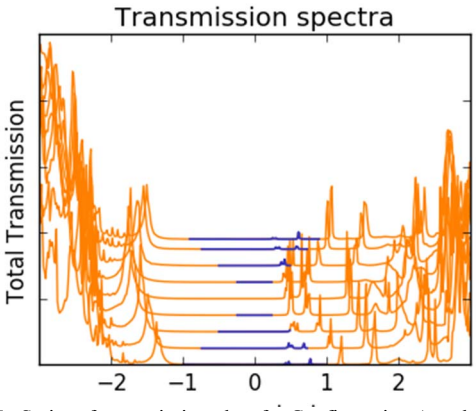


Figure 5. Series of transmission plots for Configuration A under different applied bias from -2.0V to 2.0V. From top to bottom, the blue line illustrates the applied bias window at -2.0V, -1.5V, -1.0V, -0.5V, 0V, +0.5V, +1.0V, +1.5V, +2.0V.

$$I = \frac{2e}{h}\int T(\varepsilon)[f_L(\varepsilon) - f_R(\varepsilon)]\, d\varepsilon \qquad (1)$$

where h is Planck's constant, T(ε) is the transmission function, $f_{L/R}$ is the Fermi function for left and right contacts respectively, and ε is the energy window due to the applied bias. This demonstrates how the transmission spectra at different bias can be a useful tool for explaining the $I_D$-$V_D$ characteristics of molecular junctions.

Fig. 6 shows a schematic for a conceptual flash storage device. To investigate the potential application of POM based molecular memories, the DFT simulations were linked to the device simulations by extracting the LUMO level positioning (in terms of energy position) and molecular geometry as input parameters for our in-house device simulator -NESS. The energy position of the LUMO level with respect to the conduction band of $SiO_2$ is vital for calculating the retention time of molecular flash memories which is described in Fig.6 The POM layer consists of a 3 x 3 array of $[W_{18}O_{54}(SO_3)_2]^{-4}$ molecules which stores the charge in the working device.

Fig. 7 shows the link between the $V_T$ and emission time of POM based flash memory. The KMC simulation models the change in $V_T$ over time due to the emission of electrons from the POM storage centre. Fig. 7 shows the results of 75 KMC simulations where we consider a different probability and order of discharging each POM in the gate oxide.

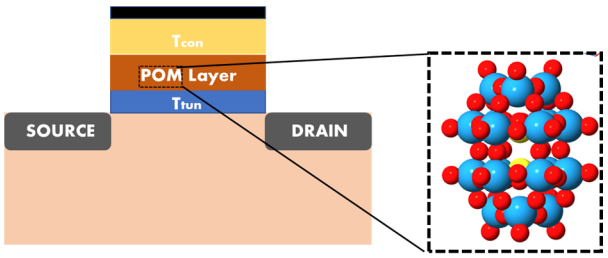


Figure 6. Conceptual device architecture for molecule-based charge trap flash memory cell. The POM cluster ($[W_{18}O_{54}(SO_3)_2]^{-4}$) is also illustrated where S=Yellow, W=Blue and O=Red.

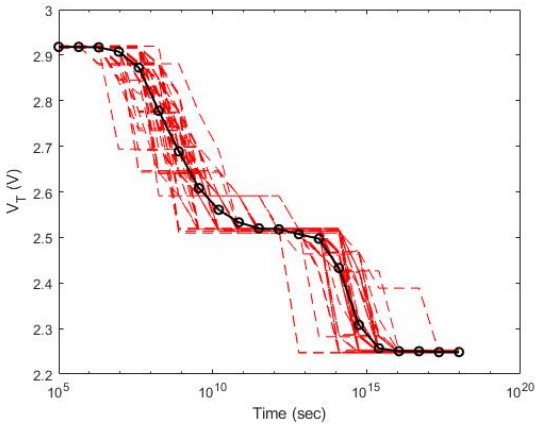


Figure 7. Threshold Voltage ($V_T$) as a function of time using Kinetic Monte Carlo in order to estimate retention time. The red is for each of the 75 devices. The black is the mean (average) change in $V_T$ vs time.

The retention time is the time it takes for the device to emit 90% of the stored electrons in the POM layer. These simulations suggest that the device will retain charge for approximately $10^8$ seconds until emissions occur and $10^{15}$ seconds to empty the storage layer. This simulated retention time meets the industry standard ten-year criteria for commercial flash memory. However, it must be noted that there is considerable statistical variation between individual KMC simulations with regards to retention time. Further study is required to optimize the device. Nonetheless these results show promise for suitable flash memory retention time.

In addition to the retention time, the plateau like feature in Fig.7 illustrates where all the POMs have lost an electron and each POM is in a 1x oxidised state. This highlights the stable redox capabilities of POM and shows potential for multi-bit storage.

## CONCLUSIONS

This work has combined first-principle modelling techniques with mesoscopic device simulation (KMC approach) to give insight into the transport properties of a POM molecule and their potential application as a floating gate in modern flash memory devices.

By using DFT and NEGF approaches the link between molecular junction geometry, contact strength and the transport properties of a POM molecule have been explored. It is evident that stronger contact with electrodes increases the available conductance channels and thus increases the current under an applied bias. It was also highlighted how different molecule geometry affects the alignment of the energy levels and thus the transmission modes leading to different current characteristics.

The calculations showed that the "horizontal" A configuration (see Fig. 1) of POM is most favorable for electron transport and shows the lowest resistance and the highest current. The theoretically calculated current is in the nA region which highlights the relatively low current flow through POM molecule in comparisons to solid state semiconductors or conductors. However, this relative higher resistance is advantageous for holding electron and thus consistent with their potential application in memory devices.

In addition to the calculations from first principles, we have combined it with mesoscopic device calculations using our in-house simulator NESS. Kinetic Monte Carlo simulations were carried out to estimate the retention time of POM based Molecular Flash memory. From an average of 75 simulations, our results demonstrate that the flash cell can hold data for up to 10 years as well as showing promising multi-bit storage.

## REFERENCES

[1] R. K. Cavin, P. Lugli, and V. V. Zhirnov, "Science and engineering beyond moore's law," *Proc. IEEE*, vol. 100, no. SPL CONTENT, pp. 1720–1749, 2012, doi: 10.1109/JPROC.2012.2190155.

[2] M. Thoss and F. Evers, "Perspective: Theory of quantum transport in molecular junctions," *J. Chem. Phys.*, vol. 148, no. 3, 2018, doi: 10.1063/1.5003306.

[3] J. Maassen, M. Harb, V. Michaud-Rioux, Y. Zhu, and H. Guo, "Quantum transport modeling from first principles," *Proc. IEEE*, vol. 101, no. 2, pp. 518–530, 2013, doi: 10.1109/JPROC.2012.2197810.

[4] L. Vilà-Nadal *et al.*, "Towards polyoxometalate-cluster-based nano-electronics," *Chem. - A Eur. J.*, vol. 19, no. 49, pp. 16502–16511, 2013, doi: 10.1002/chem.201301631.

[5] V. P. Georgiev, S. M. Amoroso, L. Vila-Nadal, C. Busche, L. Cronin, and A. Asenov, "FDSOI molecular flash cell with reduced variability for low power flash applications," *Eur. Solid-State Device Res. Conf.*, pp. 353–356, 2014, doi: 10.1109/ESSDERC.2014.6948833.

[6] C. Busche *et al.*, "Design and fabrication of memory devices based on nanoscale polyoxometalate clusters," *Nature*, vol. 515, no. 7528, pp. 545–549, 2014, doi: 10.1038/nature13951.

[7] S. Smidstrup *et al.*, "QuantumATK: An integrated platform of electronic and atomic-scale modelling tools," *J. Phys. Condens. Matter*, vol. 32, no. 1, 2020, doi: 10.1088/1361-648X/ab4007.

[8] X. López, J. J. Carbó, C. Bo, and J. M. Poblet, "Structure, properties and reactivity of polyoxometalates: A theoretical perspective," *Chem. Soc. Rev.*, vol. 41, no. 22, pp. 7537–7571, 2012, doi: 10.1039/c2cs35168d.

[9] M. Schlipf and F. Gygi, "Optimization algorithm for the generation of ONCV pseudopotentials," *Comput. Phys. Commun.*, vol. 196, pp. 36–44, 2015, doi: 10.1016/j.cpc.2015.05.011.

[10] S. Berrada *et al.*, "Nano-electronic Simulation Software (NESS): a flexible nano-device simulation platform," *J. Comput. Electron.*, vol. 19, no. 3, pp. 1031–1046, 2020, doi: 10.1007/s10825-020-01519-0.

[11] O. Badami *et al.*, "Multiscale modeling of charge trapping in molecule based flash memories," *Int. Conf. Simul. Semicond. Process. Devices, SISPAD*, vol. 2019-Septe, pp. 6–9, 2019, doi: 10.1109/SISPAD.2019.8870518.

[12] H. Basch, R. Cohen, and M. A. Ratner, "Interface geometry and molecular junction conductance: Geometric fluctuation and stochastic switching," *Nano Lett.*, vol. 5, no. 9, pp. 1668–1675, 2005, doi: 10.1021/nl050702s.

[13] Y. Xue and M. A. Ratner, "Theoretical principles of single-molecule electronics: A chemical and mesoscopic view," *Int. J. Quantum Chem.*, vol. 102, no. 5 SPEC. ISS., pp. 911–924, 2005, doi: 10.1002/qua.20484.

[14] D. Xiang, X. Wang, C. Jia, T. Lee, and X. Guo, "Molecular-Scale Electronics: From Concept to Function," *Chem. Rev.*, vol. 116, no. 7, pp. 4318–4440, 2016, doi: 10.1021/acs.chemrev.5b00680.

[15] S. Datta, *Quantum Transport: Atom to Transistor*. New York: Cambridge Univ. Press, 2005.